REFERENCES AND NOTES

1. S. Ramon y Cajal, *Histologie du Systeme Nerveux de l'Homme et des Vertebres* (Consejo Superior de Investigaciones Cientificas, Madrid, 1909), vol. 1, p. 657.
2. J. Dodd and T. M. Jessell, *Science* **242**, 692 (1988).
3. J. A. Davies, G. M. W. Cook, C. D. Stern, R. J. Keynes, *Neuron* **4**, 11 (1990); J. A. Raper and J. P. Kapfhammer, *ibid.*, p. 21; E. C Cox, B. Müller, F. Bonhoeffer, *ibid.*, p. 31.
4. M. Tessier-Lavigne, M. Placzek, A. G. S. Lumsden, J. Dodd, T. M. Jessell, *Nature* **336**, 775 (1988).
5. A. G. S. Lumsden and A M. Davies, *ibid.* **306**, 786 (1983), *ibid.* **323**, 538 (1986); J. Bolz, N Novak, M. Gotz, T. Bonhoeffer, *ibid.* **346**, 359 (1990); C. D. Heffner, A. G. S. Lumsden, D. D. M. O'Leary, *Science* **247**, 217 (1990). No chemoattractive or chemorepulsive factors have been identified yet. The use of the term factor in this report does not deny the possibility of multiple diffusive mechanisms.
6. S. A. Bayer, *Exp. Brain Res.* **50**, 329 (1983), J. E. Schwob and J. L. Price, *J Comp Neurol.* **223**, 117 (1984) The olfactory cortex of the adult anterio-ventral telencephalon receives direct input from the LOT and comprises, rostral to caudal, the anterior olfactory nucleus, piriform cortex, olfactory tubercle, cortical nucleus of the amygdala, and lateral entorhinal cortex.
7. For the tracing of axons, forebrains were dissected from E14.5 to E15.5 embryos and, after removal of the meninges, immersion-fixed in 4% paraformaldehyde in phosphate buffer at room temperature for 3 hours. Day E0 is defined by the appearance of the vaginal plug. The fluorescent tracer DiI (1% in dimethylformamide, Molecular Probes) was injected into the medial aspect of the olfactory bulb. Two to 3 days later olfactory bulbs were removed and sectioned horizontally into two pieces, flat-mounted in *p*-phenylenediamine (pH 8 in glycerol), and examined under green filtered ultraviolet light.
8. Explants of olfactory bulb, septum, olfactory cortex, and cerebral cortex were dissected from E14.5 to E15 embryos (and from E18 embryos for the olfactory cortex) in cold Eagle's minimum essential medium (Gibco). Explants that were positioned between 100 μm and ~1 mm apart in collagen-gel matrices were incubated for 40 to 48 hours in Dulbecco's modified Eagle's medium plus glutamine (Gibco) with 10% fetal calf serum for 40 to 48 hours at 37°C in a 5% CO_2 atmosphere and photographed in phase contrast.
9. T. A. Schonfeld, L. McKerracher, R. Obar, R. B. Vallee, *J. Neurosci.* **9**, 1712 (1989).
10. J. Dodd, S. B. Morton, D. Karagogeos, M. Yamamoto, T. M. Jessell, *Neuron* **1**, 105 (1988).
11. M. Yamamoto, A. M. Boyer, J. E. Crandall, M. Edwards, H. Tanaka, *J. Neurosci.* **6**, 3576 (1986).
12. For the tracing of axons in culture, DiI (1% in dimethylformamide) was injected into axons of cultures fixed in situ and left at room temperature for 2 to 3 days. Gels were removed, flat-mounted, and visualized as described above.

13. I thank J. Dodd, in whose laboratory these studies were started during a Medical Research Council Traveling Fellowship, for antibody 1C12; A. Aguayo, in whose laboratory some preliminary experiments were continued; A. McLaren, J. L. Price, S. P. Hunt, and A. Pearce-Kelly for helpful comments; L. McKerracher for antibody to MAP 1b; D. Griffin and S. P. Hunt for help with confocal microscopy, and B. Byrne for typing the manuscript.

30 June 1992; accepted 11 March 1993

A Processing Stream in Mammalian Visual Cortex Neurons for Non-Fourier Responses

Yi-Xiong Zhou and Curtis L. Baker, Jr.*

Mammalian striate and circumstriate cortical neurons have long been understood as coding spatially localized retinal luminance variations, providing a basis for computing motion, stereopsis, and contours from the retinal image. However, such perceptual attributes do not always correspond to the retinal luminance variations in natural vision. Recordings from area 17 and 18 neurons of the cat revealed a specialized nonlinear processing stream that responds to stimulus attributes that have no corresponding luminance variations. This nonlinear stream acts in parallel to the conventional luminance processing of single cortical neurons. The two streams were consistent in their preference for orientation and direction of motion but distinct in processing spatial variations of the stimulus attributes.

The receptive fields of simple cells in the early visual cortex consist of elongated, alternating excitatory and inhibitory regions. Selectivity for stimulus orientation and spatial frequency is conventionally explained in terms of linear spatial summation: only those stimuli whose luminance variations match the layout of antagonistic receptive field regions will produce a response (*1*). The wide range of preferred spatial frequencies of cortical neurons has supported a theoretical view of early vision in terms of local (piecewise) Fourier analysis (*2*). However, this scheme cannot explain visual responses to motion, stereopsis, edges, and spatial position when these attributes do not correspond to the Fourier spatial frequency power of the stimuli (*3*). One stimulus that reveals the existence of "non-Fourier" processing is an envelope stimulus, which consists of a noise pattern or a high spatial frequency luminance grating (carrier) whose contrast is modulated by a low spatial frequency pattern (envelope). Because there is no Fourier component corresponding to the pattern modulation, the detection of envelope patterns suggests the existence of nonlinear processing in the visual system (*4*). The nonlinear analysis may occur after the cortical spatial frequency–selective filtering, or before, as a consequence of early nonlinearity (*5*).

We determined whether area 17 and 18 neurons responded to spatially one-dimensional envelope stimuli (*6*), using single stationary high spatial frequency (f_c) luminance gratings as the carriers and single moving low spatial frequency (f_e) sine waves as the envelopes (Fig. 1A). Such envelope stimuli were perceived as a moving pattern of spatially alternating transparency and occlusion placed on a high spatial frequency luminance grating. The stimuli were generated by the multiplication of two grating patterns (carrier times envelope; Fig. 1B). In the Fourier frequency domain, such envelope stimuli consisted of a linear sum of three components closely centered about the high spatial frequency carrier: a stationary middle component at the carrier spatial frequency (f_c), a low side band ($f_c - f_e$), and a high side band ($f_c + f_e$) (Fig. 1C). The two side bands moved oppositely at the same temporal frequency as the envelope (f_t). However, no Fourier energy was at the envelope spatiotemporal frequency (f_e,f_t) (Fig. 1C). When a neuron responded to an envelope stimulus in which all the Fourier components were clearly outside its frequency-selective range and only the envelope spatiotemporal frequency was inside, this neuron must have been responding to the envelope of the stimulus as a result of nonlinear processing (*7*).

Thirty-nine of 94 cells responded significantly to the non-Fourier envelope pattern (*8*), although the envelope response was weaker than the same cell's luminance grating response at its optimal spatial frequency. Half of the simple (n = 22) and most of the complex (70%, n = 30) type cells in area 18 were envelope-responsive, whereas only 1 out of 12 simple and a minority of complex (20%, n = 30) cells in area 17 were envelope-responsive (*9*). Envelope-responsive cells showed the same preferred direction, degree of temporal modulation, and preferred orientation to envelope patterns as they showed to luminance grating stimuli (*10*).

The simplest explanation of such responses would be an early nonlinear transform (Fig. 2A) in which any stimulus goes through a pointwise nonlinearity (*11*) before spatial frequency–selective filtering. In this model, the nonlinearity produces a Fourier component (distortion product) at the envelope spatiotemporal frequency, and the subsequent frequency filtering picks out the distortion product and removes the

Y.-X. Zhou, Department of Psychology, McGill University, Montreal, Quebec, Canada H3A 1B1.
C. L. Baker, Jr., McGill Vision Research Unit, Ophthalmology Department, McGill University, Montreal, Quebec, Canada H3A 1A1.

*To whom correspondence should be addressed.

high-spatial-frequency ($>f_c$) components in the stimulus. Because there is no spatial frequency–selective filtering before the nonlinearity, this hypothesis predicts that a wide range of changes in the carrier spatial frequency should not affect the strength of envelope responses. In addition, the envelope spatial frequency tuning should be the same as that for single luminance gratings in a given neuron because both the distortion product and the luminance grating responses are processed by the same filter.

In order to test these predictions, we used two kinds of stimuli: (i) conventional luminance grating stimuli with only one Fourier frequency component and (ii) envelope stimuli (Fig. 1) with three Fourier frequency components. The luminance spatial frequency dependence of a neuron was measured with luminance grating stimuli at several spatial frequencies. Then the dependence on carrier spatial frequency was determined with envelope stimuli in which the envelope spatial frequency was fixed at the optimal luminance spatial frequency while the carrier spatial frequency was varied. Without exception (n = 39), the carrier spatial frequency dependence for an envelope-responsive neuron was found to be selective to a narrow range of high spatial frequencies (*12*) that was much higher than the selective range for luminance gratings (Fig. 3A). The two spatial frequency–selective ranges did not overlap, except for one cell. We then examined 14 of these neurons for their dependence on envelope spatial frequency. In most cases (n = 11), the envelope and luminance spatial frequency tuning curves were different: the

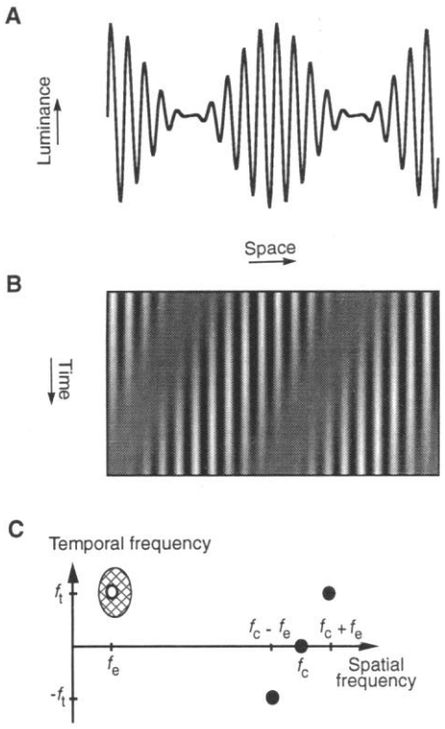

Fig. 1. Spatially one-dimensional envelope stimuli. (**A**) A luminance profile of the stimulus at a given time. (**B**) The space-time intensity plot of a stimulus. The abscissa is spatial position, the ordinate is time, and the gray level indicates the luminance at a given spatial position and time. In this example, the contrast envelope moves leftward while the carrier remains stationary. (**C**) The power spectrum of the stimuli; symmetric left-side quadrants are omitted. Three Fourier components (solid circles) were in the spectrum, but no Fourier component was at the envelope spatiotemporal frequency (open circle). The hatched area indicates the neuron's frequency-selective range for single luminance gratings. The temporal frequency of the drifting envelope was set to the optimal for the drifting luminance grating (f_t).

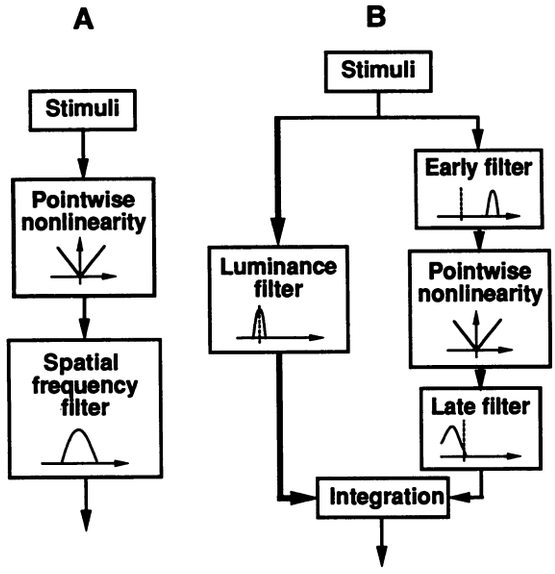

Fig. 2. (**A**) The "early nonlinear" hypothesis. (**B**) Proposed "two-stream" mechanism. The left stream is for luminance processing, and the right one is for envelope processing. The heavy arrow indicates a stronger response in the luminance than in the envelope stream. The icon in each filter box depicts the filter's tuning curve on a logarithmic spatial frequency scale, and the icons in the nonlinearity boxes indicate full-wave rectification.

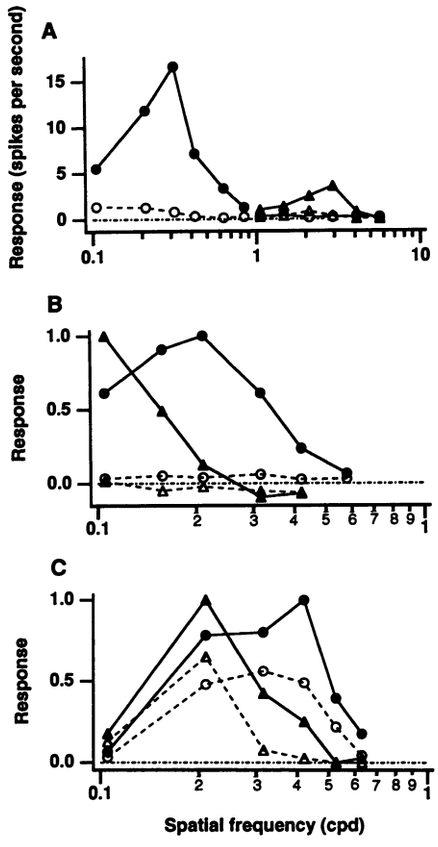

Fig. 3. Dependence of neuronal response to envelope stimuli on the carrier and envelope spatial frequency. Responses to the stimulus moving in the preferred direction of the cell (solid lines and symbols) and to the nonpreferred direction of motion (dashed lines and open symbols) are shown. The measured value of spontaneous activity was subtracted from all the responses. The abbreviation "cpd" stands for cycles per degree of visual angle. (**A**) Dependence on the carrier spatial frequency. Two kinds of spatial frequency tuning curves measured on the same neuron are illustrated: (i) the luminance spatial frequency tuning curve (●, ○), measured from the responses to single luminance gratings, and (ii) the carrier spatial frequency tuning curve (▲, △) from the envelope responses. The envelope spatial frequency was held constant at the cell's optimal luminance spatial frequency (0.3 cpd), and the abscissa indicates the carrier spatial frequency of the envelope stimuli. (**B** and **C**) Dependence on the envelope spatial frequency for two other neurons. Two spatial frequency tuning curves are plotted in each graph: (i) the luminance spatial frequency tuning curve (●, ○) and (ii) the envelope spatial frequency tuning curve (▲, △) in which the carrier spatial frequency was fixed at the cell's optimal value [1.42 cpd for (B) and 2.73 cpd for (C), obtained from the measurement of the cell's carrier spatial frequency dependence as in (A)]. Curves in (B) and (C) were normalized to the largest value in the preferred direction response curve.

preferred range of envelope spatial frequency was lower than that of luminance spatial frequency (Fig. 3, B and C).

The frequency-selective nature of the carrier spatial frequency dependence and the discrepancy between envelope and luminance spatial frequency dependences rule out the possibility of explaining the envelope responses by any early pointwise nonlinearity (Fig. 2A). Instead we propose a special processing stream (Fig. 2B, right side) that is parallel to the luminance processing (Fig. 2B, left side) in the receptive field organization. This envelope-responsive stream can be modeled by three stages: (i) early spatial frequency filtering selective to a narrow range of high frequency, providing the carrier spatial frequency dependence; (ii) pointwise nonlinearity; and (iii) late spatial frequency filtering, which corresponds to the envelope spatial frequency dependence. Consider an envelope stimulus with a carrier spatial frequency inside the selective range of the early filter and with its envelope spatial frequency inside the selective range of the late filter. The Fourier components (close to the carrier frequency) in the stimulus are passed by the early filter. The nonlinearity produces a Fourier component (envelope component) at the envelope spatiotemporal frequency. This Fourier component is then picked up by the late filter, allowing the neuron to respond to the envelope stimulus. Notice that the envelope-responsive stream does not respond to luminance grating stimuli: since the spatial frequency–selective ranges of the early and late filters do not overlap, any luminance grating stimulus cannot pass both the early and the late filters. To account for the cell's luminance response properties, a separate luminance-processing stream (Fig. 2B, left side) is still needed.

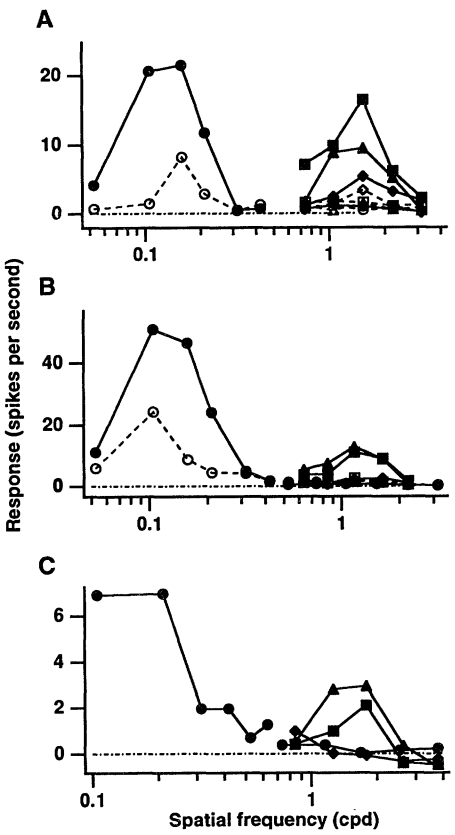

Fig. 4. Carrier spatial frequency tuning curves of three neurons, measured with various envelope spatial frequencies. The conventions for symbols and axes are the same as in Fig. 3A, unless indicated. (**A** and **B**) Two directionally biased neurons. The luminance spatial frequency tuning curves are indicated by (●, ○). Three carrier spatial frequency tuning curves for each graph were measured with the envelope spatial frequencies 0.05 cpd (▲, △), 0.1 cpd (■, □), and 0.2 cpd (◆, ◇). (**C**) A nondirectionally biased cell. Only the responses to one direction of stimulus motion are plotted. Three envelope spatial frequencies [0.1 cpd (▲), 0.2 cpd (■), and 0.3 cpd (◆)] were used in measuring the carrier spatial frequency tuning curves.

Because separate filters mediate the registration of Fourier energy in the envelope stimuli and the extraction of the envelope component, the three-stage cascade model predicts a separable dependence on the carrier and envelope spatial frequencies; changing the envelope spatial frequency should not affect the shape and range of the carrier spatial frequency dependence. Fourteen envelope-responsive cells were examined for their dependence on carrier spatial frequency under a series of envelope spatial frequencies. Varying the envelope spatial frequency affected only the magnitude of the carrier spatial frequency tuning without changing its shape and optimal frequency (Fig. 4), demonstrating separable carrier and envelope spatial frequency dependencies (as predicted by Fig. 2B).

These findings indicate that contrast envelope detection is functionally important and not an "accidental" secondary consequence of imperfections in an otherwise linear mechanism. The proposed two-stream model supplements a conventional linear-filter model with a parallel, nonlinear pathway. Such an arrangement permits the robust detection of moving, oriented contours in a manner invariant with their composition. The lack of correspondence between spatial frequency selectivity for luminance and envelope gratings seems puzzling but supports the distinct nature of envelope information. Further studies on interactions between the two pathways may shed light on the functional importance of this discrepancy.

REFERENCES AND NOTES

1. The receptive fields of complex type cells are generally thought to be composed of subunits similar to simple cells; J. A. Movshon, I. D. Thompson, D. J. Tolhurst, *J. Physiol.* (*London*) **283**, 53, 79 (1978); H. Spitzer and S. Hochstein, *Prog. Neurobiol.* **31**, 285 (1988).
2. E. W. Campbell and J. G. Robson, *J. Physiol.* (*London*) **197**, 551 (1968); J. G. Robson, in *Visual Coding and Adaptability*, C. S. Harris, Ed. (Erlbaum, Hillsdale, NJ, 1980), pp. 177–214; D. G. Albrecht, R. L. De Valois, L. G. Thorell, *Science* **207**, 88 (1980); R. M. Shapley and P. Lennie, *Annu. Rev. Neurosci.* **8**, 547 (1985).
3. C. Redies, J. M. Crook, O. D. Creutzfeldt, *Exp. Brain. Res.* **61**, 469 (1986); A. Toet and J. J. Koenderink, *Vision Res.* **28**, 133 (1988); C. Chubb and G. Sperling, *J. Opt. Soc. Am. A* **5**, 1986 (1988); in *Proceedings: 1989 IEEE Workshop on Visual Motion* (IEEE Computer Society Press, Washington, DC, 1989), pp. 126–138; E. Peterhans and R. von der Heydt, *Trends Neurosci.* **14**, 112 (1991); H. R. Wilson, R. Blake, D. L. Halpern, *J. Opt. Soc. Am. A* **8**, 229 (1991); T. D. Albright, *Science* **255**, 1141 (1992); D. H. Grosof, R. M. Shapley, M. J. Hawken, *Invest. Ophthalmol. Visual Sci.* (suppl.) **33**, 1257 (1992); R. F. Hess and I. E. Holliday, *Vision Res.* **32**, 1085 (1992); J. C. Boulton and C. L. Baker, *ibid.*, in press.
4. G. B. Henning, B. G. Hertz, D. E. Broadbent, *Vision Res.* **15**, 887 (1975); A. M. Derrington and D. R. Badcock, *ibid.* **25**, 1869 (1985); J. Nachmias, *ibid.* **29**, 137 (1989); K. Turano and A. Pantle, *ibid.*, p. 207.
5. Such an early nonlinearity could be, for example, the logarithmic transform of the luminance information at the level of the photoreceptors or the half-wave rectification in cells of the lateral geniculate nucleus [G. J. Burton, *Vision Res.* **13**, 1211 (1973); A. M. Derrington, *ibid.* **27**, 1377 (1987); B. Chen, W. Makous, D. R. Williams, *ibid.* **33**, 413 (1993)].
6. Stimuli were produced with a Compaq Deskpro 386 microcomputer controlling a Revolution graphics board (Number Nine Corp.) and were displayed on a Joyce screen (spatial resolution, 512 pixels by 256 pixels; temporal resolution, 5.2 ms per frame; mean luminance, 115 cd/m^2; display size, 30 cm by 23 cm; viewing distance, 57 cm for area 17 recordings, 114 cm for area 18 recordings). A contrast of 77% was used for all the stimuli. The Joyce screen's internal feedback-corrected z-amplifier provided intensity linearization such that the contrast of the distortion product from the envelope stimuli was less than 0.6% {highest contrast sensitivity of the cat is 1% at 0.5 cpd [R. Blake, S. J. Cool, M. L. J. Crawford, *Vision Res.* **14**, 1211 (1974)]}. Three lines of evidence indicated that the distortion product did not contribute substantially to the neuron's envelope responses. First, the envelope responses were significantly larger than the response to a 0.6% contrast luminance grating at the cell's optimal spatial frequency. Second, the envelope responses were abolished when the screen was covered by a diffusing sheet, which provided strong attenuation to high spatial frequencies (about 80% at the optimal carrier frequency), and very little to low frequencies (<5% at the envelope frequency). If the neurons had been responding to any screen distortion product, covering the screen with a diffusing sheet should not have affected the responses. Third, if a screen nonlinearity had contributed substantially to the envelope responses, the envelope-responsive properties should have followed the predictions from the early nonlinear hypothesis, which was rejected by the results of this investigation (see text).
7. Our investigation of envelope responses should not be confused with that of D. A. Pollen, J. P. Gaska, and L. D. Jacobson [*Vision Res.* **28**, 25 (1988)], in which the carrier spatial frequency of their envelope stimuli was inside the neuron's luminance spatial frequency–selective range and only complex cells responded to the temporal profile of the envelope patterns.
8. Conventional procedures for animal surgery, anesthesia, optical refraction, and electrophysiology have been described elsewhere [C. L. Baker, Jr., *Visual Neurosci.* **4**, 101 (1990)] and were in ac-

cordance with the institutional guidelines of McGill University. Briefly, surgical anesthesia was obtained with 2.5% intravenous sodium thiopentone. Anesthesia and paralysis were maintained during recording with 7:3 NO_2/O_2, sodium pentobarbital (1 mg per kilogram of body weight per hour), and gallamine triethiodide (10 mg/kg per hour). End-tidal CO_2, temperature, electroencephalogram, and electrocardiogram were monitored and maintained at normal levels. Cells were classified as simple or complex according to conventional criteria [D. H. Hubel and T. N. Wiesel, *J. Physiol. (London)* **160**, 106 (1962); B. C. Skottun *et al.*, *Vision Res.* **31**, 1079 (1991)]. A statistical significance test was used to compare each neuron's envelope response with its spontaneous activity and luminance response at the carrier spatial frequency.

9. Because the envelope-responsive cells included both simple and complex types, the nonlinearity mediating the envelope response must be distinct from the one distinguishing complex cells from simple cells.
10. In testing the envelope responses at different stimulus orientations, the carrier and envelope were always at the same orientation.
11. A pointwise nonlinearity is defined as: output(x,t) = N[input(x,t)] (x, distance; t, time). Candidates for such a transform include half-wave or full-wave rectification, a squaring operation, a logarithmic transformation, or any pointwise nonlinearity that can be expressed by a polynomial function with nonzero even terms.
12. D. G. Albrecht and R. L. De Valois [*J. Physiol. (London)* **319**, 497 (1981)] did not observe envelope-responsive cells in striate cortex of cat and monkey, using envelope stimuli with a fixed 5:1 ratio for carrier:envelope spatial frequency and a rigid motion between envelope and carrier. Our investigation indicated that this ratio varied from 4 to 30 for different neurons. Consequently, fixing the frequency ratio at 5:1 significantly reduced the chance of finding envelope-responsive cells, especially considering the small sample size (n = 24), the smaller percentage of envelope-responsive neurons in area 17 of cat (see text), and the very narrow range of effective carrier frequency for a given neuron.
13. We thank R. F. Hess for suggestions on the manuscript and M. Moscovitch for contributions to computer programming. Supported by the Canadian Medical Research Council (MA-9685) and Stairs Memorial grants to C.L.B. Gallomine triethiodide was donated by Rhone-Poulenc Pharma.

21 December 1992; accepted 20 April 1993

G Protein–Coupled Signal Transduction Pathways for Interleukin-8

Dianqing Wu, Gregory J. LaRosa, Melvin I. Simon*

Interleukin-8 (IL-8) is one of the major mediators of the inflammatory response. The pathways by which IL-8 activates inositide-specific phospholipase C (PLC) were investigated by co-expression of different components of the guanosine triphosphate binding protein (G protein) pathway in COS-7 cells. Two distinct IL-8 receptors reconstituted ligand-dependent activation of endogenous PLC when transfected together with the G protein α subunits $G\alpha_{14}$, $G\alpha_{15}$, or $G\alpha_{16}$. However, reconstitution was not observed with cells that overexpressed $G\alpha_q$ or $G\alpha_{11}$. Furthermore, IL-8 receptors interacted with endogenous pertussis toxin–sensitive G proteins or with the recombinant G protein G_i to release free βγ subunits that could then specifically activate the β2 isoform of PLC. These findings suggest that IL-8 acts through signal-transducing pathways that are limited to specific heterotrimeric G proteins and effectors. These may provide suitable targets for the development of anti-inflammatory agents.

A wide range of chemical signals are transduced into intracellular changes in metabolism through the coupling of receptors to heterotrimeric guanosine triphosphate (GTP) binding proteins (G proteins). The interaction of ligand with a G protein–coupled membrane receptor results in the exchange of guanosine diphosphate (GDP) bound to the G protein α subunit for GTP, which causes the subsequent dissociation of the heterotrimer into the α and βγ subunits (*1*, *2*). To examine the nature of the signal transduction pathways that take part in complex cellular responses such as inflammation, we sought to reconstitute signal transduction with white cell–specific receptors and to examine their requirements for specific G proteins and specific effectors. The peptide cytokine IL-8 is one of the most potent chemoattractants for neutrophils (*3*). IL-8 also induces angiogenesis, mediates cytokine-induced transendothelial neutrophil migration (*4*), and triggers a variety of other effects associated with the inflammatory response (*3*). The complementary DNAs (cDNAs) that encode two distinct types of IL-8 receptors, designated α and β, have been cloned and sequenced (*5–7*). These receptors appear to couple to G proteins and activate PLC in neutrophils (*3*).

The G_q class of G protein α subunits can activate members of the β family of PLC isozymes to stimulate the release of inositides and diacylglycerol (*8*). Five cDNAs that encode these α subunits of this class have been characterized: $G\alpha_q$, $G\alpha_{11}$, $G\alpha_{14}$, $G\alpha_{15}$, and $G\alpha_{16}$ (*2*). All of the α subunits activate the PLC-β1 isoform (*9*, *10*), and most of them activate the PLC-β2 isoform (*10*, *11*). Furthermore, the free βγ complex activates PLC-β2 but not PLC-β1 in cotransfection assays (*12*) and preferentially activates PLC-β2 in cell-free assays (*13*). The responses of cells to ligands that induce PLC activity have been divided into two groups: those that are sensitive to pertussis toxin inhibition and those that are resistant (*2*). Pertussis toxin covalently modifies certain Gα subunits so that ligand-induced exchange of GDP for GTP on the Gα subunit is blocked. Pertussis toxin–resistant activation of PLC is probably mediated by the α subunits of the G_q class. The $G\alpha_q$ subunits that activate PLC-β lack a site for modification by pertussis toxin (*2*), and a variety of specific antisera to the $G\alpha_q$ subunits block receptor-mediated responses that are resistant to pertussis toxin (*14*). The pertussis toxin–sensitive response can be reconstituted through receptor-mediated release of βγ subunits from members of the G_i class (*12*). The toxin apparently blocks the activation of PLC-β2 by interfering with the release of the βγ subunits from the trimeric G proteins.

The expression of PLC-β2 appears to be developmentally regulated and is expressed in the hematopoietic lineage (*15*). Expression of certain Gα subunits, such as $G\alpha_{16}$, is limited to cells derived from the hematopoietic lineage (*16*). To determine whether the two IL-8 receptors, IL-8Rα and IL-8Rβ, transduce signals through any of the known G_q family members, we cotransfected COS-7 cells with cDNAs encoding IL-8Rα or IL-8Rβ alone or together with $G\alpha_q$, $G\alpha_{11}$, $G\alpha_{14}$, $G\alpha_{15}$, or $G\alpha_{16}$. Neither nontransfected COS-7 cells (Fig. 1) nor cells transfected with receptors alone showed any ligand-induced release of inositol phosphates (Fig. 1, A and B). However, ligand-induced release of inositol phosphates was detected in cells that co-expressed IL-8Rα or IL-8Rβ and $G\alpha_{16}$ or $G\alpha_{14}$ but not in cells cotransfected with either of the IL-8 receptors and $G\alpha_q$ or $G\alpha_{11}$. This indicates that both IL-8 receptors can activate PLC molecules that are endogenous to COS-7 cells by specifically coupling to $G\alpha_{14}$ and $G\alpha_{16}$ but not to $G\alpha_q$ or $G\alpha_{11}$. Tests with specific antibodies indicated that PLC-β1 was present in COS-7 cells but PLC-β2 was not (*12*). Both IL-8 receptors can also couple to $G\alpha_{15}$ (Fig. 1, A and B), the mouse counterpart of human $G\alpha_{16}$ (*17*). The dose-dependent responses to ligand indicate a mean effective concentration (EC_{50}) for both IL-8Rα and IL-8Rβ of about 2.5 nM (Fig. 1C), which is very close to the inhibition constant of IL-8 for

D. Wu and M. I. Simon, Division of Biology, 147-75, California Institute of Technology, Pasadena, CA 91125.
G. J. LaRosa, Repligen Corporation, Department of Molecular Biology, 1 Kendall Square, Cambridge, MA 02132.
*To whom correspondence should be addressed.